

# Optically induced three-dimensional photonic lattices and quasi-crystallographic structures

Julian Becker<sup>a,\*</sup>, Jolly Xavier<sup>b</sup>, Martin Boguslawski<sup>a</sup>, Patrick Rose<sup>a</sup>, Joby Joseph<sup>b</sup>,  
and Cornelia Denz<sup>a</sup>

<sup>a</sup>Institut für Angewandte Physik and Center for Nonlinear Science, Westfälische  
Wilhelms-Universität Münster, Correnstr. 2/4, 48149 Münster, Germany;

<sup>b</sup>Indian Institute of Technology Delhi, Hauz Khas, New Delhi-110016, India

## ABSTRACT

We present an experimental investigation of the formation of three-dimensional (3D) nonlinear photonic lattices. They are optically induced inside an externally biased cerium doped strontium barium niobate (SBN) photorefractive crystal by a single step multiple beam interference approach. An easy implementation of this scheme using a spatial light modulator (SLM) is demonstrated making the induced structures effortlessly reconfigurable and allowing for a rich variety of two or three dimensional periodic and quasi-periodic crystallographic structures. We show an analysis of these nonlinear photonic lattices based on plane wave guiding, momentum space spectroscopy, and far field diffraction pattern imaging.

**Keywords:** complex photonic lattices, quasi-crystals, three-dimensional gratings, optical induction, photorefractive nonlinearity

## 1. INTRODUCTION

Two- and three-dimensional photonic crystals offer new possibilities to route, control, and steer light in all-optical information processing and nanophotonic devices. Therefore, materials with periodic refractive index modulations have become the subject of extensive research for several years now.<sup>1,2</sup> While different fabrication methods, such as lithography or direct laser writing, have been utilized to produce permanently fixed periodic structures, some future applications certainly require an increased flexibility and the possibility to tune and adapt photonic lattices in real-time. Especially the fabrication of 3D quasi-crystallographic complex structures of higher rotational symmetry remains a real challenge, as many of the conventional methods become either technically unsuitable or extremely complicated. This makes the approach of a reconfigurable optical induction method in photorefractive materials particularly attractive.<sup>3,4</sup>

In contrast to well-studied two-dimensional structures,<sup>5–10</sup> we now focus on the investigation of the formation of three-dimensional, optically induced photonic lattices with periodic or quasi-crystallographic structure as well as their distinct properties. In order to create three-dimensional interference patterns we employ a versatile method based on advanced wave front phase-only spatial light modulation. This approach gives rise to three-dimensional refractive index gratings inside a photorefractive SBN:Ce crystal. One of the advantages of our technique is that it is not limited to conventional periodic crystal lattices, but can easily be extended to quasi-crystallographic structures, i.e. structures demonstrating long-range order and sharp diffraction peaks. Experimentally, we analyze the induced 3D lattices using different methods including plane-wave diffraction, momentum space spectroscopy, and far field diffraction pattern imaging.

## 2. OPTICAL INDUCTION

It has been shown that using multiple beam interference or multiple exposure to two-beam interference all fourteen Bravais lattices could be generated.<sup>11,12</sup> Recently, various optical induction based fabrication approaches have been adapted to fabricate 2D<sup>8,9</sup> as well as 3D<sup>13–16</sup> periodic or quasi-periodic structures in different photosensitive materials. Unlike conventional multiple beam interference, where a complicated optical setup needs

---

\*Send correspondence to J. B., julian.becker@uni-muenster.de

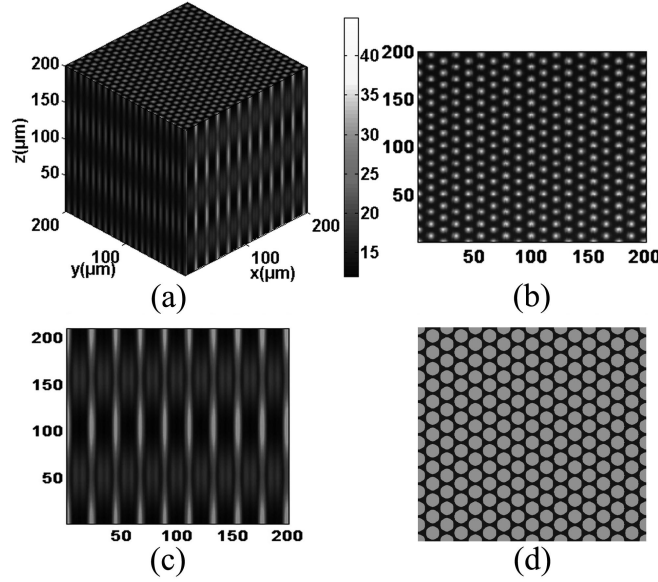


Figure 1. (a)–(c) Computer simulation of the light intensity distribution of the lattice-forming beams. (a) 3D interference pattern formed by  $(6 + 1)$  beam configuration. (b), (c) Light intensity distribution, respectively, in the  $xy$ - and  $xz$ -plane. (d) Computed phase engineered pattern to generate the seven lattice-forming beams.

to be implemented, recently, the actual techniques make use of diffractive optical elements, the single prism method, or a spatial light modulator assisted approach.<sup>17–19</sup>

Taking advantage of the wavelength sensitivity of a particular photorefractive medium, optically induced photonic lattices can be generated at very low power levels. Making use of the versatility of a programmable SLM,<sup>7,19,20</sup> we base our technique on computer generated reconfigurable phase engineered patterns. Thus, we greatly simplify the conventional multiple beam interference technique for 3D photonic structures. The computer engineered phase pattern, representing the phase information extracted from the overall complex amplitude of the irradiation profile of the interference pattern for a particular 3D photonic lattice structure, is sent to a programmable phase-only SLM. This phase engineered pattern spatially modulates an incident plane-wave, thus generating the required lattice-forming beams.

Various 3D lattice-forming geometries for different reconfigurable 3D periodic lattices with variable periodicity can be experimentally investigated by this versatile approach. For an  $n$ -fold three-dimensional axial photonic quasi-crystal the spatial intensity distribution of  $(n + 1)$  plane waves is given by

$$I(\mathbf{r}) = \sum_{i=0}^n |\mathbf{E}_i|^2 + \sum_{i=0}^n \sum_{\substack{j=0 \\ j \neq i}}^n \mathbf{E}_i \mathbf{E}_j^* e^{i(\mathbf{k}_i - \mathbf{k}_j) \cdot \mathbf{r} + i(\psi_i - \psi_j)}. \quad (1)$$

Here,  $\mathbf{E}_i$ ,  $\mathbf{k}_i$  and  $\psi_i$  are respectively the complex amplitudes, wave vectors, and initial phase offsets of the interfering beams. A whole family of quasi-crystallographic structures can be obtained by choosing an interference between one central beam  $\mathbf{E}_0 e^{ikz}$  and  $n$  beams with coplanar wave vectors (i.e. the projections of the beams' wave-vectors on the  $xy$ -plane all lie on a circle) of the form

$$\mathbf{k}_i = k [\cos(\phi_i) \sin(\vartheta) \mathbf{e}_x + \sin(\phi_i) \sin(\vartheta) \mathbf{e}_y + \cos(\vartheta) \mathbf{e}_z], \quad \phi_i = \frac{2\pi i}{n}, \quad \forall i = 1, \dots, n. \quad (2)$$

The characteristic length scale of the intensity modulation is determined by the angle  $\vartheta$  between the central beam and the side beams. More particularly, we get truly periodic structures for  $n \in \{2, 3, 4, 6\}$  whereas for  $n = 5$  or  $n > 6$  we obtain quasi-crystallographic structures. The presence of the additional central beam is responsible for a modulation along the  $z$ -direction. Leaving it out gives rise to  $z$ -invariant intensity distributions.

To generate the beams at the desired angles and with the prescribed phase offsets  $\phi_i$ , we calculate the phase distribution of the entire complex light field in the  $xy$ -plane and use it to modulate an incoming plane wave with the SLM. All the undesired components of the phase-engineered light-field generated by the SLM can be filtered out e.g. utilizing a mask placed in the focal plane of a consecutive telescope (cf. Sect. 3).

In Fig. 1 we exemplify the explained induction technique by showing the simulated intensity distributions for a regular 3D hexagonal structure by interference of  $(6+1)$  beams.

### 3. EXPERIMENTAL SETUP

In our optical setup (cf. Fig. 2) a frequency-doubled Nd:YAG laser ( $\lambda = 532$  nm) is first split up into two beams using a combination of a beam splitter and a half-wave plate, allowing for intensity adjustments at the same time. One of the subsequent arms is used for the writing and the other one for spectroscopic testing of the three-dimensional lattice. They are operated one at a time only, while the other one is blocked by a shutter.

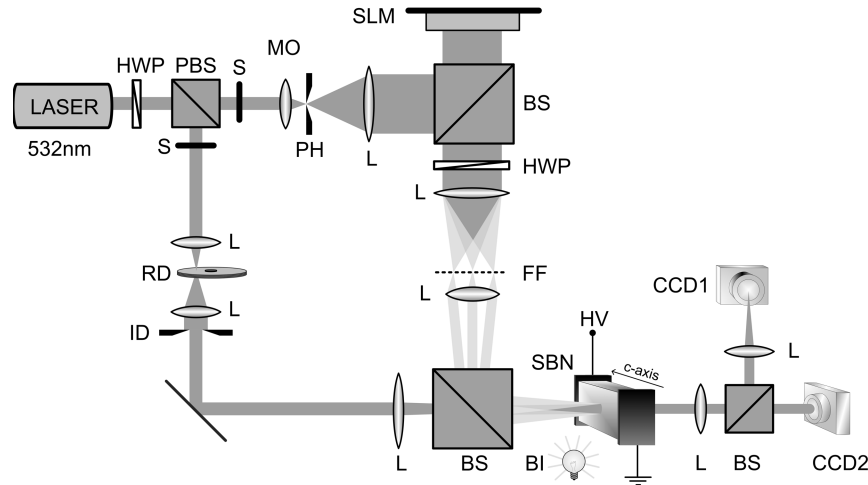


Figure 2. Schematic sketch of the experimental setup. BI: background illumination, CCD: Camera, FF: Fourier mask, HV: high-voltage source, HWP: half-wave plate, ID: iris diaphragm, L: lens, MO: microscope objective, (P)BS: (polarizing) beam splitter, PH: pinhole, RD: rotating diffuser, S: shutter, SLM: phase-only spatial light modulator.

In the writing arm, the lattice-forming beam is first expanded and spatially filtered using a microscope objective with subsequent pinhole, and a collimation lens. Then, the collimated beam is directed onto the phase-only SLM (Holoeye PLUTO-VIS), modulating the wave front according to the computer generated complex phase pattern. The SLM is imaged onto the photorefractive cerium doped  $\text{Sr}_{0.60}\text{Ba}_{0.40}\text{Nb}_2\text{O}_6$  (SBN:Ce) crystal (dimensions are  $5\text{ mm} \times 5\text{ mm} \times 20\text{ mm}$ ) using a high aperture telescope. In the focal plane of the telescope, all undesired wave vector components are blocked by appropriate Fourier filtering. The lattice wave is linearly polarized perpendicular to the  $c$ -axis of the crystal (o-polarized). Typically, the total power of the lattice wave—measured at the front face of the crystal—is about  $40\text{--}60\text{ }\mu\text{W}$ . The crystal is biased with an externally applied static electric field of  $1.5\text{ kV/cm}$ . Typical exposure times are in the order of  $60\text{--}90\text{ s}$ .

The other arm in the setup constitutes a standard momentum space spectroscopy configuration,<sup>21</sup> with a telescope and a rotating diffuser near its focal plane. The randomized light field coming out of the telescope is focused onto the front face of the crystal to excite a broad spatial spectrum of waves. The Fourier image (captured with CCD1) of the waves transmitted through the crystal gives important structural information about the actually induced lattice (cf. Sect. 4). The second camera captures the real space image of the crystal's back face.

On the one hand, for the formation of the lattices an o-polarized beam is used to avoid feedback of the induced structures on the lattice-forming light field. The analysis on the other hand is performed with extraordinary polarization. Due to the higher relevant electro-optic coefficient the probe beam then experiences a significant refractive index contrast.

#### 4. EXPERIMENTAL RESULTS

An experimental analysis of the fabricated 3D hexagonal lattice is given in Fig. 3 (cf. also Fig. 1). The biased crystal has been illuminated with the o-polarized lattice beam from the SLM for about a minute. After this writing time the lattice beam is blocked. The shutter of the spectroscopy arm of the setup was closed during the induction process.

Figure 3(a) gives the image of the guided wave intensity acquired using CCD2. Here, the lattice is illuminated with a plane wave (no phase pattern on the SLM). This is accomplished by reducing the power of the beam to only a fraction of the writing power and turning its polarization by  $90^\circ$ , so that it is e-polarized now. Imaging the crystal's back face, the transmitted intensity distribution qualitatively maps the refractive index modulation induced by the lattice-forming wave, thus effectively imaging the photonic lattice in that direction.

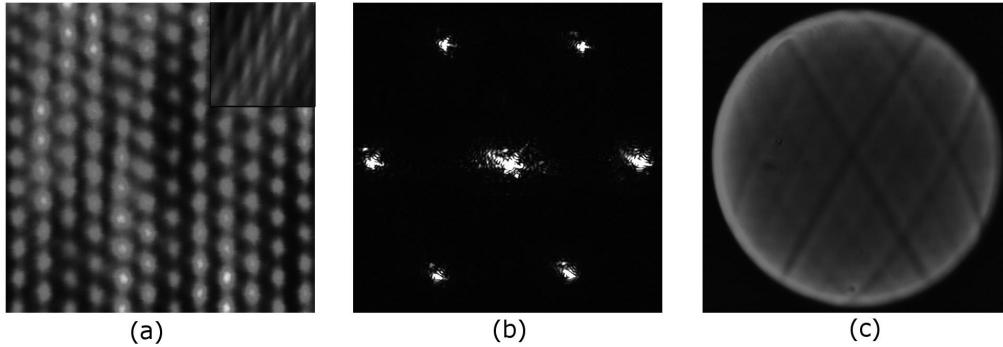


Figure 3. Three-dimensional hexagonal lattice in photorefractive SBN:Ce. (a)  $xy$ -plane of the photonic lattice formed by an o-polarized lattice wave ( $xz$ -plane is given in the inset). (b) Far-field diffraction pattern. (c) Momentum space spectroscopic image.

To ensure detailed visualization of the 3D lattice formed, the image of the  $xz$ -plane is taken after rotating the crystal with the induced photonic lattice inside by  $90^\circ$  (cf. inset in Fig. 3(a)). Together with the obtained results for the  $xy$ -plane, the presence of a distinct modulation also in the  $xz$ -plane documents a truly three-dimensional optically induced photonic lattice structure inside the photorefractive SBN crystal. The generated hexagonal photonic lattice structure has a lattice period of  $14\ \mu\text{m}$  and in the direction of propagation the lattice period is measured to be  $25\ \mu\text{m}$ .

Now imaging the Fourier plane using CCD1, we obtain the far field diffraction pattern of the lattice (Fig. 3(b)), which again demonstrates the hexagonal structure, by giving six pronounced diffraction peaks.

In Fig. 3(c) we see the result of the momentum space spectroscopy of the induced 3D hexagonal structure. During this analysis, the writing arm is blocked and the lattice is probed with the spectroscopy arm of the setup using e-polarized light. The resulting image shows several dark lines, characteristic of the induced lattice, which appear due to Bragg reflections in the corresponding directions. Here, we are also able to recognize the anisotropic nature of the grating by the absence of certain expected dark lines parallel to the crystal's  $c$ -axis. This anisotropy originates from the photorefractive nonlinearity in SBN, which is dominated by the drift of charge carriers along the direction of the applied external electric field. Modulations perpendicular to this direction are subsequently suppressed and the corresponding dark lines disappear.<sup>7, 21</sup>

One of the major technological advantages of our approach is that it is not limited to conventional periodic crystal lattices alone, but can easily be extended to arbitrary, also non-periodic structures. Among them, quasi-crystal structures play an important role, i.e. structures demonstrating long range order and sharp diffraction peaks. We demonstrate the generation of well-defined reconfigurable 3D quasi-crystallographic nonlinear photonic structures with various rotational symmetries up to 32-fold quasi-crystals. Several examples of some high-symmetry quasi-crystallographic structures are shown in Fig. 4, which are almost impossible to generate using the conventional multiple beam interference approaches.

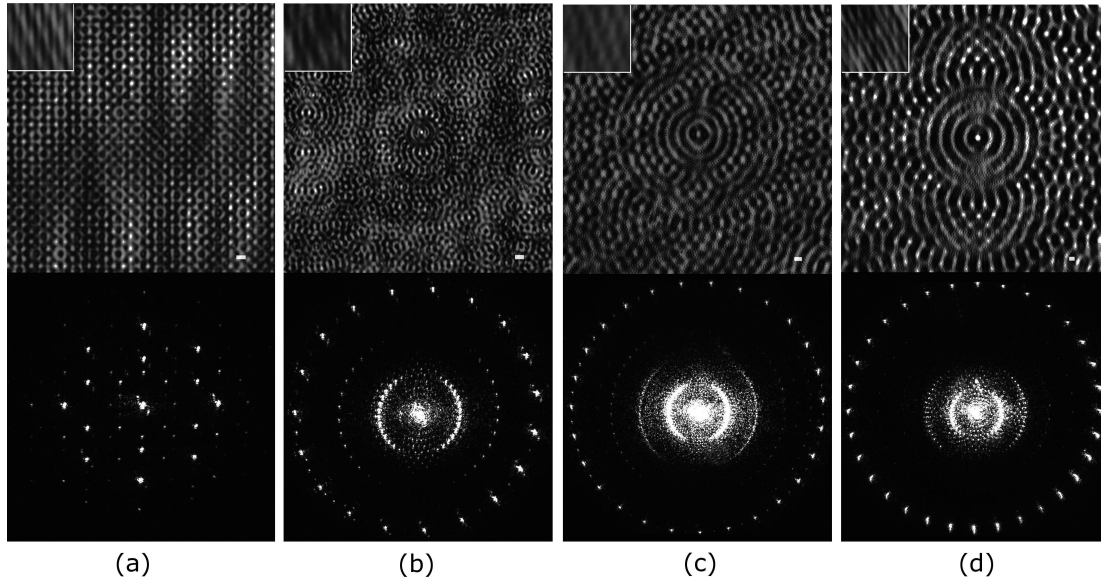


Figure 4. Upper row: Recorded images of  $xy$ -plane of 3D axial photonic quasi-crystals fabricated in an externally biased SBN:Ce photorefractive crystal. The recorded images of a portion of the  $xz$ -plane of the structures, containing a region near to the propagation axis, are shown in the inset. Lower row: Far field diffraction pattern belonging to the corresponding structure in the upper row. Three-dimensional axial photonic quasi-crystals with (a) 8-fold, (b) 19-fold, (c) 27-fold, and (d) 32-fold rotational symmetry: All scale bars equal  $10\ \mu\text{m}$ .

## 5. CONCLUSION

In conclusion, we have demonstrated a versatile approach for the fabrication of large area 3D photonic quasi-crystallographic structures by a single step optical induction approach. By means of computer-engineered reconfigurable phase patterns, lattice-forming beams are generated to fabricate 3D periodic as well as quasi-crystallographic structures belonging to various rotational symmetries. The structures can be written, erased and reconfigured with ease in almost real-time, which suggests potential applications in nonlinear photonic devices.

## REFERENCES

- [1] Joannopoulos, J. D., Johnson, S. G., and Winn, J. N., [*Photonic Crystals – Molding the flow of light*], Princeton University Press, Princeton NJ (2008).
- [2] Yablonovitch, E., Gmitter, T. J., and Leung, K. M., “Photonic band structure: The face-centered-cubic case employing nonspherical atoms,” *Phys. Rev. Lett.* **67**(17), 2295–2298 (1991).
- [3] Xavier, J., Rose, P., Terhalle, B., Joseph, J., and Denz, C., “Three-dimensional optically induced reconfigurable photorefractive nonlinear photonic lattices,” *Opt. Lett.* **34**(17), 2625–2627 (2009).
- [4] Xavier, J., Boguslawski, M., Rose, P., Joseph, J., and Denz, C., “Reconfigurable optically induced quasicrystallographic three-dimensional complex nonlinear photonic lattice structures,” *Adv. Mat.* **22**(3), 356–360 (2010).
- [5] Terhalle, B., Träger, D., Tang, L., Imbrock, J., and Denz, C., “Structure analysis of two-dimensional nonlinear self-trapped photonic lattices in anisotropic photorefractive media,” *Phys. Rev. E* **74**(5), 057601 (2006).
- [6] Desyatnikov, A. S., Sagemerten, N., Fischer, R., Terhalle, B., Träger, D., Neshev, D. N., Dreischuh, A., Denz, C., Krolkowski, W., and Kivshar, Y. S., “Two-dimensional self-trapped nonlinear photonic lattices,” *Opt. Express* **14**(7), 2851–2863 (2006).
- [7] Terhalle, B., Desyatnikov, A. S., Bersch, C., Träger, D., Tang, L., Imbrock, J., Kivshar, Y. S., and Denz, C., “Anisotropic photonic lattices and discrete solitons in photorefractive media,” *Appl. Phys. B* **86**(3), 559–559 (2007).

- [8] Wang, X., Tam, W., Chan, C., and Sheng, P., "Large-area two-dimensional mesoscale quasi-crystals," *Adv. Mat.* **15**(18), 1526–1528 (2003).
- [9] Zito, G., Piccirillo, B., Santamato, E., Marino, A., Tkachenko, V., and Abbate, G., "Two-dimensional photonic quasicrystals by single beam computer-generated holography," *Opt. Express* **16**(8), 5164–5170 (2008).
- [10] Freedman, B., Bartal, G., Segev, M., Lifshitz, R., Christodoulides, D. N., and Fleischer, J. W., "Wave and defect dynamics in nonlinear photonic quasicrystals," *Nature* **440**, 1166–1169 (2006).
- [11] Cai, L. Z., Yang, X. L., and Wang, Y. R., "All fourteen bravais lattices can be formed by interference of four noncoplanar beams," *Opt. Lett.* **27**(11), 900–902 (2002).
- [12] Dwivedi, A., Xavier, J., Joseph, J., and Singh, K., "Formation of all fourteen bravais lattices of three-dimensional photonic crystal structures by a dual beam multiple-exposure holographic technique," *Appl. Opt.* **47**(12), 1973–1980 (2008).
- [13] Bitá, I., Choi, T., Walsh, M. E., Smith, H. I., and Thomas, E. L., "Large-area 3d nanostructures with octagonal quasicrystalline symmetry via phase-mask lithography," *Adv. Mat.* **47**(19), 1403–1407 (2007).
- [14] Wang, X., Xu, J., Lee, J., Pang, Y., Tam, W., Chan, C., and Sheng, P., "Realization of optical periodic quasicrystals using holographic lithography," *Appl. Phys. Lett.* **88**(5), 051901 (2006).
- [15] Lai, N. D., Lin, J. H., Huang, Y. Y., and Hsu, C. C., "Fabrication of two- and three-dimensional quasi-periodic structures with 12-fold symmetry by interference technique," *Opt. Express* **14**(22), 10746–10752 (2006).
- [16] Xu, J., Ma, R., Wang, X., and Tam, W. Y., "Icosahedral quasicrystals for visible wavelengths by optical interference holography," *Opt. Express* **15**(7), 4287–4295 (2007).
- [17] Xu, D., Chen, K. P., Ohlinger, K., and Lin, Y., "Holographic fabrication of diamondlike photonic crystal template using two-dimensional diffractive optical elements," *Appl. Phys. Lett.* **93**(3), 031101 (2008).
- [18] Sun, X. H., Tao, X. M., Ye, T. J., Xue, P., and Szeto, Y., "Optics design and fabrication of 3D electrically switchable hexagonal photonic crystal," *Appl. Phys. B* **87**(1), 65–69 (2007).
- [19] Jenness, N. J., Wulff, K. D., Johannes, M. S., Padgett, M. J., Cole, D. G., and Clark, R. L., "Three-dimensional parallel holographic micropatterning using a spatial lightmodulator," *Opt. Express* **16**(20), 15942–15948 (2008).
- [20] Rose, P., Terhalle, B., Imbrock, J., and Denz, C., "Optically induced photonic superlattices by holographic multiplexing," *J. Phys. D: Appl. Phys.* **41**(22), 224004 (2008).
- [21] Bartal, G., Cohen, O., Buljan, H., Fleischer, J. W., Manela, O., and Segev, M., "Brillouin zone spectroscopy of nonlinear photonic lattices," *Phys. Rev. Lett.* **94**(16), 163902 (2005).